

# The Interaction of Slag and Carbon on the Electrical Properties



Gerrit R. Surup, Kseniia Koseniuk, and Merete Tangstad

**Abstract** Renewable reducing agents are intended to replace significant amounts of fossil-fuel-based reductants in submerged arc furnaces in the upcoming decades. In this study, the interaction of a manganese slag to a charcoal, a semi-coke, and a metallurgical coke was investigated. In a first series, the wettability of the slag was measured, while the electrical resistivity of carbon particles was measured by a four-point measuring technique. It was shown that the contact resistant between the carbon materials significantly decreased by void and pore filling. The results were validated by measuring the bulk resistivity of carbon-slag blended bed. While the slag is nonconductive below melting temperature, electrical current is highly conducted in the molten phase. The higher electrical resistivity of charcoal compared to the fossil-fuel-based reductants improves the local heat generation in the carbon bed, concomitant reducing the viscosity of the slag, which may be beneficial for tapping of the furnace. While the work described here is not specifically on furnace tapping, the work is linked to good furnace operation, hence indirectly relevant.

**Keywords** Charcoal · Coal char · Metallurgical coke · Ferromanganese slag · Wettability · Electrical resistivity

## Introduction

The increasing average living standard and demand for metals can hamper the aim to be climate neutral by 2050. Industrialized countries are expected to adjust their economies to be greenhouse gas (GHG) neutral by the middle of the century, by which time a transition from fossil-fuel-based technologies to renewables can decrease current anthropogenic CO<sub>2</sub> emissions; the metallurgical industry will play an important role in decarbonization, yet it also needs to reduce its carbon emissions. The

---

G. R. Surup (✉) · K. Koseniuk · M. Tangstad  
Norwegian University of Science and Technology (NTNU), 7491 Trondheim, Norway  
e-mail: [gerrit.r.surup@ntnu.no](mailto:gerrit.r.surup@ntnu.no)

M. Tangstad  
e-mail: [merete.tangstad@ntnu.no](mailto:merete.tangstad@ntnu.no)

Norwegian process industry estimated a reduction of  $\approx 75\%$  CO<sub>2</sub> emissions which could potentially be achieved by the use of biomass and its derivatives [1].

A large portion of special elements is required for alloying steels. While on average about 3–5% of alloying elements are used in steel production, high alloy steels can contain more than 12% alloying elements [2]. Most of these elements are produced by carbothermal or electrolytic production, for example, in blast furnaces, submerged arc furnaces (SAF), electric arc furnaces (EAF), or in electrolytic cells. Reduction of metal oxides to the metallic form in SAF and EAF is carried out by solid carbon, such as woodchips, charcoal, coal, anthracite, or metallurgical coke.

Carbon reductants in SAF operations have two main purposes: 1. to reduce the metal oxides and quartz to the metallic form and 2. to form a conductive bed to conduct current and provide the necessary heat through the Joule effect. The electrical resistivity of carbon materials is essential to ensure a stable operation of the SAF, in which more than 50% of the required thermal energy is provided by electrical power [3]. While several publications deal with the use of raw carbon materials [4–7], only limited knowledge of wetted coke beds or the interaction between renewable reductants and slag has been published.

In SAF and EAF, electrical energy dissipation occurs by both micro-arcing and resistive heating, for example, there is less than 5% arcing occurring in chrome production [8], with up to 15% occurring in silicomanganese production [9]. Silicon and ferrosilicon, on the other hand, exhibit much larger electrical dissipation by arcing, in which a crater below the electrode tips is formed, transferring between 20 and 60% of the electrical energy [8]. Thus, the electrical properties of the carbon bed are important in order to maintain stable heat generation and operation of SAFs.

In this study, the interaction between ferromanganese (FeMn) slag and charcoal was investigated and compared to blends of FeMn slag to coal char and metallurgical coke. Blends of fossil-fuel-based carbon reductants and high-carbon ferrochromium have shown that the electrical resistivity is significantly affected by the volume fraction of slag [10].

Similar results were obtained for blends of metallurgical coke and charcoal at low temperatures [11]. The aim of this study was to investigate: (1) the behavior of charcoal, coal char and metallurgical coke towards FeMn slag; (2) determine the slag intrusion into packed carbon beds; and (3) to measure the electrical resistivity of partially wetted carbon beds. In this paper, wetted carbon refers to a carbon bed that is in contact with a molten slag.

## Materials and Methods

A metallurgical coke, a coal char and an industrial charcoal were selected as representative carbon materials for examining the behavior of an FeMn slag produced in a pilot test. The coal char and industrial charcoal were obtained from a local silicon producer, while the metallurgical coke was the same as used in the production of ferromanganese. The carbon material also had been used in a previous study and had

**Table 1** Proximate and ultimate analyses of carbon feedstocks

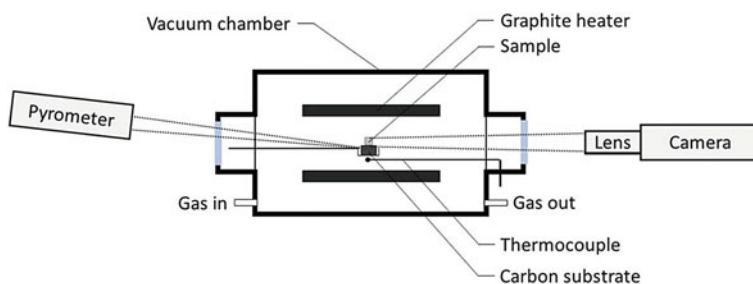
	Unit	Metallurgical coke	Charcoal	Coal
Moisture	wt%, ar	<0.1	0.9	0.6
Ash	wt%, db	12.1	2.4	3.8
Volatile matter	wt%, db	<0.5	<0.5	<0.5
Carbon content	wt%, daf	98.9	99.1	99.2
Hydrogen content	wt%, daf	<0.1	<0.1	<0.1
Nitrogen content	wt%, daf	<0.5	<0.5	<0.5
Oxygen content	wt%, daf	<0.5	<0.5	<0.5
Sulfur content	wt%, daf	0.3	–	0.3

*ar* As received basis, *db* dry basis, *daf* dry ash free basis

been heat treated to 1650 °C [7]. The analyses of the carbon feedstocks after heat treatment are summarized in Table 1.

### Sessile Drop Test

Prior to each experiment, the crushed slag sample was split using a sample splitter, ground to a particle size less than 100  $\mu\text{m}$ , and then compacted to form a small cylinder (diameter: 4 mm; height: 4–5 mm). The cylinder was placed on the carbon substrate (graphite, charcoal, coal char, or metallurgical coke), which had been heat treated at 1600 °C prior to the experiment. The specimen was placed on the sample arm and positioned in the center of the sessile drop furnace, schematically shown in Fig. 1. The chamber was closed, evacuated to less than 0.3 mbar, and consecutively purged by 0.15 l  $\text{min}^{-1}$  of argon to render the chamber inert. The furnace was heated at a heating rate of 300 K  $\text{min}^{-1}$  to 900 °C and further heated at a constant heating rate of 10 K  $\text{min}^{-1}$  to a final temperature of 1700 °C. At temperatures above 900 °C, the substrate temperature was measured by a pyrometer in addition to the furnace

**Fig. 1** Schematic of the sessile drop test

temperature, which was measured by a thermocouple type C. After the heating cycle was completed, the sample was cooled to room temperature, the sample and substrate removed and stored in sample containers.

The sessile drop test was carried out to determine the interaction between the manganese slag and the different carbon substrates, as well as the ash fusion temperatures, which are composed of the deformation temperature (IDT), softening temperature (ST), hemispheric temperature (HT), and flow temperature (FT, also called fluid temperature). The sample and substrate were cast in iodized resin, cut, and further investigated by scanning electron microscopy.

### *Slag Intrusion Measurement*

The interaction of the slag and the dry carbon bed (coke bed) was determined at temperatures up to 1550 °C in an argon atmosphere. Carbon fines with a particle size less than 2 mm were blended with wood tar and water at a ratio of 100:35:65, homogenized and compacted inside an alumina crucible. The compacted sample was dried overnight at 105 °C to remove moisture and volatile components from the tar binder, concomitantly increasing the mechanical stability of the pellet. A channel (diameter: 2.5, 4, and 5 mm) and a chamfer of 60° were machined into the sample, schematically shown in Fig. 2a. Slag particles of 1.5–1.75 g were placed on top of the channel to simulate dense particle packing.

Three samples were placed in a graphite crucible in an induction furnace IF75 (Inductotherm Europe, Droitwich Spa, UK), as presented in Fig. 2b. Argon (purity 5.0) was purged continuously at a constant flow rate of 1 l min<sup>-1</sup> to render the atmosphere in the crucible inert. The furnace control thermocouple was positioned

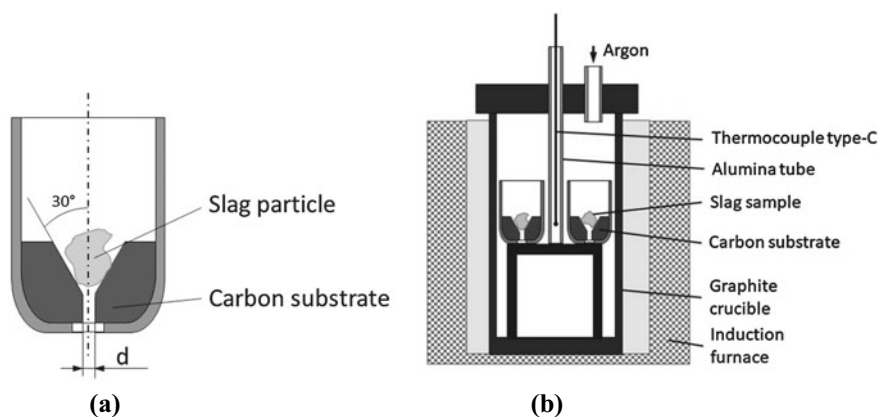
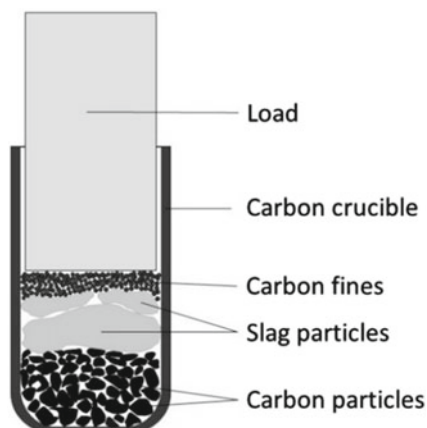


**Fig. 2** Schematic of the slag intrusion experiment. **a** Compacted carbon material with defined chamfer and channel and **b** installed setup in induction furnace

**Fig. 3** Schematic of the load introduced intrusion experiment



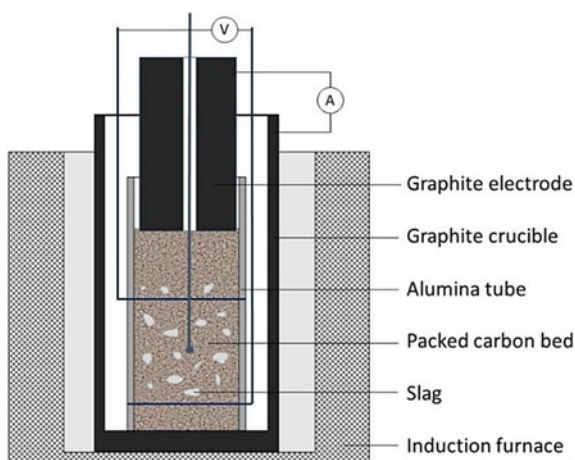
at the sample height to minimize any temperature gradient between the furnace and sample. The furnace was heated at a heating rate of  $15 \text{ K min}^{-1}$  to  $900 \text{ }^\circ\text{C}$  and kept at this temperature for 10 min to minimize the temperature gradient in the sample. The sample was subsequently heated to  $1550 \text{ }^\circ\text{C}$  at a constant heating rate of  $10 \text{ K min}^{-1}$  and kept at the final temperature for 30 min. After the heating program was finished, the furnace was turned off and the samples were cooled in an argon atmosphere to room temperature.

To simulate the burden load on the carbon bed in a SAF, an additional load (compaction pressure  $\approx 10 \text{ kPa}$ ) was introduced on the slag sample, schematically shown in Fig. 3. Carbon particles with particle size  $2\text{--}4.75 \text{ mm}$  were filled in a graphite crucible (height 67 mm, diameter 40 mm, wall thickness 4 mm) to a height of 30 mm and compacted by vibrating compaction. A slag layer was added above the carbon samples to a height of  $\approx 15 \text{ mm}$ . Carbon fines ( $d_p < 250 \text{ }\mu\text{m}$ ) were installed above the slag layer to ensure an evenly distribution of the additional load. The height of the load was noted and monitored over the heating program to analyze the melting and the void filling of the carbon bed. The crucible was placed in the center of the induction furnace called IF75 and heated, following the same heating procedure described in the previous paragraph.

### ***Electrical Resistivity***

Electrical resistivity measurements were performed using a four-point probe measurement system (SINTEF, Trondheim, Norway) installed in the induction furnace IF75 as described elsewhere [7]. 150 g of slag sample ( $d_p \leq 2 \text{ mm}$ ) was blended into the carbon feedstock ( $4.75 \text{ mm} \leq d_p \leq 9.5 \text{ mm}$ ) and distributed homogeneously in the measurement zone and also slightly above it, resulting in a slag carbon ratio of 7:3 for metallurgical coke, 5:3 for coal char and 1:1 for charcoal. A

**Fig. 4** Schematic of the electrical measurement setup at NTNU/SINTEF



schematic of the setup is shown in Fig. 4. The furnace was heated with a constant heating rate of  $15 \text{ K min}^{-1}$  to  $900 \text{ }^\circ\text{C}$  and kept at this temperature for 15 min to minimize the radial temperature gradient in the packed bed. Furthermore, the furnace was heated at a heating rate of  $10 \text{ K min}^{-1}$  to  $1650 \text{ }^\circ\text{C}$  and kept at that temperature for 30 min. The electrical resistivity of the packed bed was investigated for each  $25 \text{ }^\circ\text{C}$  temperature increase in the center of the bed.

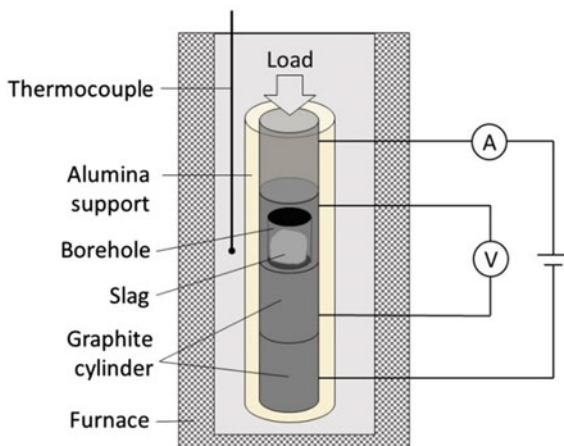
### Single Particle Interaction with Slag

The effect of slag on the contact resistance between single particles was investigated by using a graphite cylinder (diameter: 16 mm, length:  $\approx 25 \text{ mm}$ ) in the induction furnace IF75. A hole (diameter: 10 mm, depth: 15 mm) was drilled in the upper cylinder and partially filled with slag, schematically shown in Fig. 5.

### Scanning Electron Microscopy

Scanning electron microscopy was performed on the residue from sessile drop test and slag intrusion experiments using a high-resolution microscope ULTRA 55 (Zeiss, Oberkochen, Germany) under a high vacuum to investigate the change in the structure in the contact region.

**Fig. 5** Schematic of the four-point measurement of single particles



## Results and Discussion

The interaction between the slag and different carbon substrates and the ash melting behavior was investigated in the sessile drop test as shown in Fig. 6. The first ash deformation and hemispheric temperature were measured at  $\approx 1190$  °C and 1220–1240 °C, respectively. These values are generally in agreement with reported values in the literature [12]. The lower melting temperature compared to manganese ores indicates that the MnO content in the slag was reduced to  $\leq 40\%$  in the pilot-scale experiment [13]. This hemispheric shape was kept at a temperature of 1700 °C for graphite and coal substrates, whereas the slag surpassed the flow temperature for metallurgical coke and charcoal at temperatures above 1680 °C, schematically as shown in Fig. 6d, f.

A further gas formation in the slag droplet was observed for temperatures above 1300 °C for all carbon substrates, resulting in a volume increase up to 200% of its melting volume. The non-wetting behavior of graphite and carbon materials below 1600 °C and the further reduction on carbon substrates is also in agreement with information in the published literature [14, 15].

Scanning electron microscopy on a cross section of the charcoal and metallurgical coke substrates revealed that some of the slag diffused into the carbon matrix, as shown in Fig. 7. The slag intrusion into the carbon bed increases at temperatures above 1600 °C [13], in which slag reduction and a lower viscosity at elevated temperature increase the slag flow and intrusion into the void fraction and pore structure. The composition of the carbon substrate, the surface layer, and the outer slag was investigated using EDS with the results summarized in Table 2. The EDS analysis confirmed that some surface layer slag was further reduced to its metallic form, whereas the composition of the main slag droplet above the carbon substrate remained nearly constant. The EDS results for the slag intrusion experiments deviated from the results from sessile drop test by  $\leq 4\%$  points.

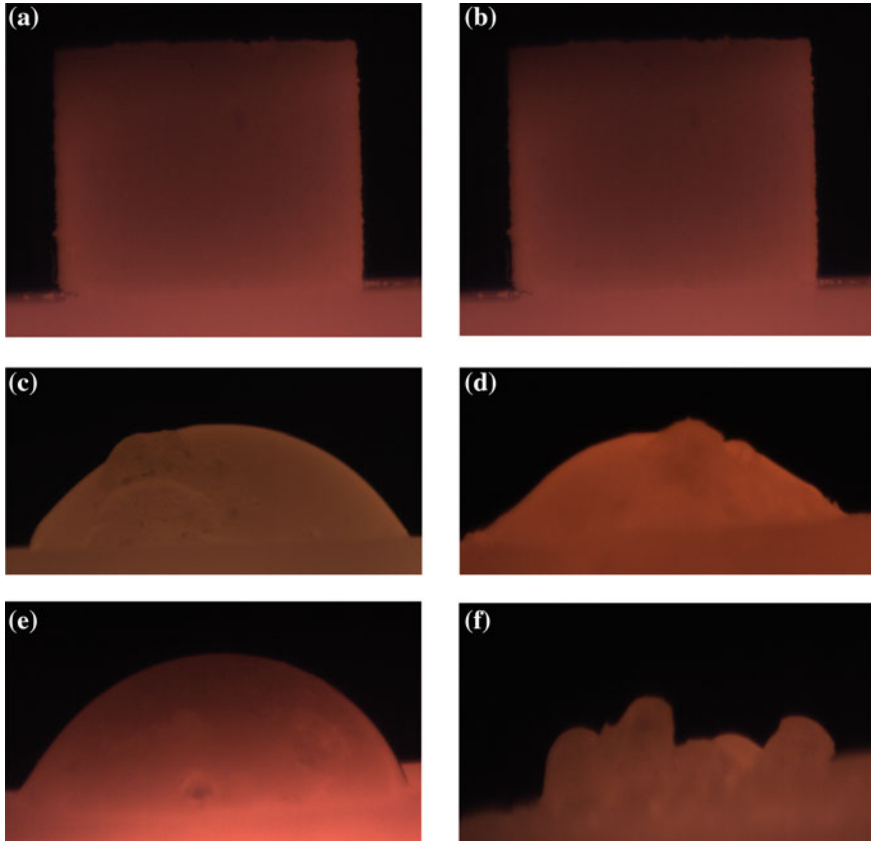


**Fig. 6** Ash–carbon interaction of FeMn slag with different carbon substrates in sessile drop test **a** First deformation at 1190 °C on graphite substrate, **b** Hemispheric temperature at 1239 °C on graphite substrate, **c** shape at 1696 °C on graphite substrate. **d** shape at 1698 °C on metallurgical coke, **e** shape at 1698 °C on coal char and **f** shape at 1699 °C on charcoal

The slag intrusion was measured for channel diameter larger of 2.5, 4, and 5 mm. At a channel diameter of 4 mm, some of the slag passed through the channels for metallurgical coke, whereas no slag flow was observed for charcoal and coal char samples. However, at a channel diameter of 5 mm, the complete slag droplets passed through the channels of all carbon substrates. The non-wetting properties of charcoal, coal char and metallurgical coke towards FeMn will decrease the slag flow into the void. However, it may be possible that small slag droplets pass into the void packed bed, inhibiting a further flow through the bed.

The burden of raw material in the SAF introduces a load on the molten slag, which can potentially press or force the molten slag into the void. However, the current experiments showed that a compaction pressure of 10 kPa was not sufficient



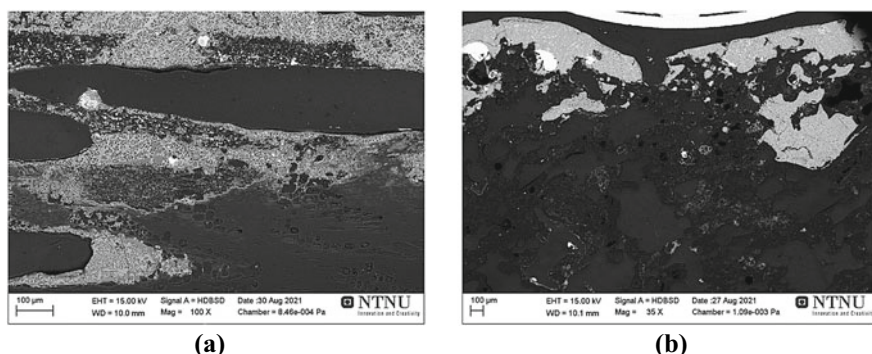


**Fig. 7** SEM images of the cross section of the carbon substrate from sessile drop test: **a** charcoal top layer and **b** metallurgical coke top layer

**Table 2** EDS spot analysis of charcoal and metallurgical coke substrate and slag from sessile drop test

Element, %/%	Charcoal substrate			Metallurgical coke substrate		
	Carbon	Surface layer	Slag	Carbon	Surface layer	Slag
C	100	13.0	8.1	98.7	18.1	8.9
O		5.8	41.4		6.3	42.1
S				0.4		
Al		0.4	8.9	0.5	0.4	8.2
Ca			9.5	0.4	1.1	11.0
Si		17.3	9.3			5.0
Mn		40.0	22.8		48.3	24.8
Fe		23.5			11.3	

to compress the molten slag into the void fraction of fines or small carbon particles (3.35–4.75 mm).

For coal char and charcoal particles, the molten slag formed an additional layer on top of the carbon bed, whereas small amounts of slag were found at the bottom of the crucible for metallurgical coke, as shown in Fig. 8. Fine particles in carbon blends can therefore hamper the slag transport in the upper region of the dry coke bed. Fine formation will increase with the addition of mechanical weak material in carbon blends, for example, charcoal in metallurgical coke.

Figure 9 presents the electrical resistivity measurements for graphite cylinders with a partial slag layer in the contact region. A graphite rod (length: 100 mm, diameter: 16 mm) was used as a reference for the material property. It is seen that the electrical resistivity further decreases at temperatures above about 1200 °C, corresponding to the partial slag melting for the top carbon particle. In addition, the electrical resistivity became more stable, in which the standard deviation of the

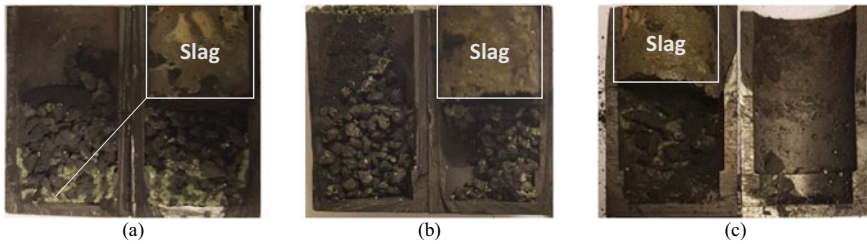


**Fig. 8** Images of **a** metallurgical coke, **b** coal char and **c** charcoal packed beds with a top layer of FeMn slag. Parts of the packed beds of charcoal were removed prior to the image to investigate possible slag intrusion in the packed bed

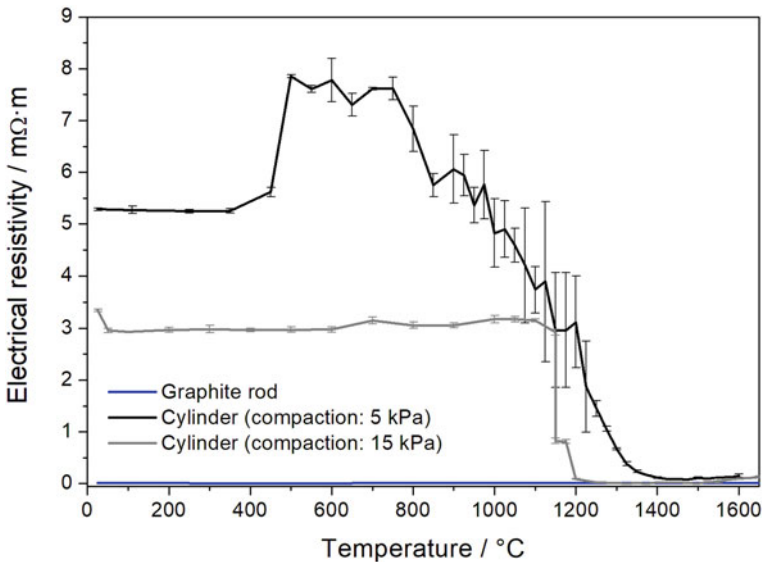


**Fig. 9** Electrical resistivity of graphite cylinders with FeMn slag at the contact area. The graphite rod was investigated to measure the electrical resistivity of the carbon material

measurements decreased by a factor of  $\geq 5$ . The large standard deviation is related to the weak contact by the low compaction pressure [7]. The increased stability and decreased electrical resistivity indicate that the compaction pressure and contact resistance are of less importance in the wetted carbon bed, respectively, that most of the electrical energy dissipation takes place in the dry coke bed.

The electrical resistivity of the carbon–FeMn slag packed beds is shown in Fig. 10. At temperatures below 1000 °C, the electrical resistivity of the carbon–slag blends was  $\approx 50\%$  larger than that of the dry carbon material, whereas a lower electrical resistivity was measured at temperatures above about 1200 °C.

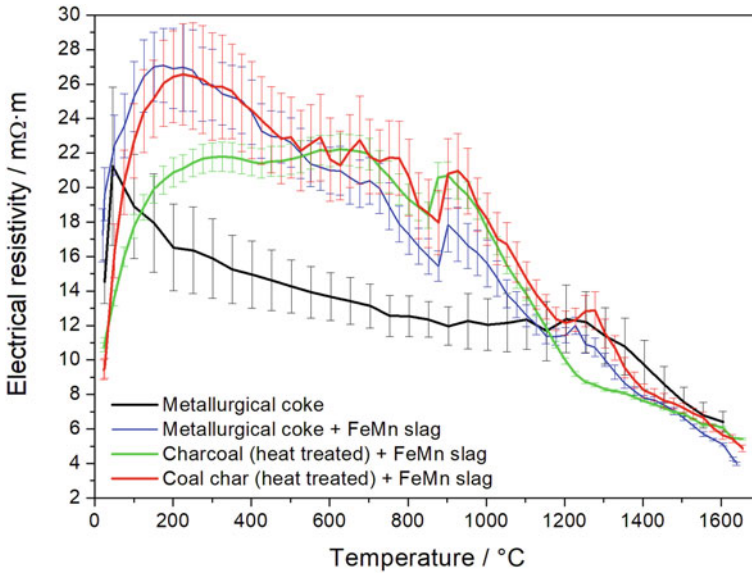


**Fig. 10** Electrical resistivity of different carbon–slag packed beds at temperatures below 1650 °C

It is hypothesized that the higher electrical resistivity is related to the replacement of carbon by slag particles, decreasing the amount of possible current paths through the packed bed [10]. At higher temperatures, the nonconductive slag becomes conductive and reduces the contact resistance between the particles.

Figure 9 also shows that the contact resistance between graphite particles was almost rendered of little consequence due to the molten slag forming between the particles at elevated temperature. COMSOL simulations have shown that the current density at the contact area of particles in wetted carbon beds is the highest at the contact point [16]. Current paths through the FeMn slag would increase the current density at the contact areas between the particles. A similar electrical resistivity of FeMn slag and metallurgical coke was reported for 1200–1400 °C, in which the electrical conductivity increases with increasing temperature [17]. However, further reactions between the molten slag and the carbon bed can result in gas formation at the contact area and may result in an interference of the current paths.

Despite the poor transport of FeMn slag in the preliminary experiments,  $\approx 33\text{--}50\%$  of the slag was recovered below the measurement zone. Thus, slag droplets, which did not coalesce with other droplets, passed through the carbon bed. In addition, some of the droplets exhibited a metallic appearance and will be further investigated. It is expected that an increased void filling of the wetted carbon bed will result in a further decrease of the electrical resistivity. An increased electrical conductivity between the carbon particles will decrease the risk of micro-arcs and arcs in the carbon bed, decreasing the energy dissipation in wetted carbon beds [9]. The investigated

carbon species resulted in a more equal electrical resistivity in the wetted carbon bed compared to the dry carbon bed, which differed by a factor of 2–3 [4, 11, 18, 19].

The results are promising in that renewable reductants (e.g., charcoal) can replace fossil-fuel-based reductants without negatively affecting the heat generation in a SAF. Heat generation in the dry carbon bed is further increased by the larger electrical resistivity of charcoal, whereas the electrical resistivity in wetted carbon beds remain nearly constant. The local heat generation near the electrodes may improve the temperature profile in a SAF, enhancing the flow properties of the slag by tapping the furnace. Furthermore, the low electrical resistivity of charcoal at temperatures less than 1000 °C will minimize possible current paths in the burden.

## Conclusion

The electrical resistivity of wetted carbon beds was measured for FeMn slag in charcoal, coal char, and metallurgical coke packed beds and was determined to 5.5–6.5 mΩ m at 1550 °C. Thus, the difference in the electrical resistivity of wetted carbon beds was reduced to less than 1 mΩ m at elevated temperature, whereas dry carbon beds can differ by more than 10 mΩ m (e.g., 6 mΩ m for metallurgical coke and 18 mΩ·m for charcoal). The slag between single particles rendered the contact resistance between the particles to a low level resulted in an electrical resistivity to be close to that of the pure material. Thus, a wetted carbon bed has a lower electrical resistance than that of the pure carbon materials in dry coke beds.

Charcoal, coal char and metallurgical coke exhibited a non-wetting behavior for temperatures less than 1650 °C. The high surface tension in combination with the not-wetting properties resulted in a minimum channel diameter of 4 mm for FeMn to pass into the void fraction. Large slag droplets and coalescence of small droplets can hinder the flow through the carbon bed and void filling. Pressure applied to the burden did not enhance the flow into a charcoal or coal char matrix, whereas small amounts of slag were recovered in the metallurgical coke bed. It was confirmed in sessile drop experiments that FeMn slag penetrated the outer layers of the carbon particles at temperatures above 1600 °C for charcoal and metallurgical coke. It is assumed that the macro-porosity of metallurgical coke and charcoal and the partial consumption of surface carbon increased the flow into the carbon matrix.

The results indicate that renewable reductants can, in all likelihood, replace fossil-fuel-based reductants in the wetted carbon bed without negatively affecting the electrical properties in the lower part of the SAF. The larger electrical resistivity of the dry carbon (charcoal) bed will further increase the heat generation close to the electrodes, possibly decreasing slag viscosity by an increased temperature.

## References

1. Norsk Industri (2016) The Norwegian process industries' roadmap-combining growth and zero emissions by 2050. Available online: <https://www.norskindustri.no/siteassets/dokumenter/rapporter-og-brosjyrer/the-norwegian-process-industries-roadmap-summary.pdf> (accessed on 10 September 2018).
2. Carvill J (1994) Mechanical engineer's data handbook, Butterworth-Heinemann, 1st(edition), p 352
3. Tangstad M (2013) Metal production in Norway, 1. ed., Akademika, p 240
4. Eidem PA, Tangstad M, Bakken JA (2007) Measurement of material resistivity and contact resistance of metallurgical coke. In: Proceedings of the INFACON XI, New Delhi, India, pp 561–571
5. Eidem P, Tangstad M, Bakken J (2008) Determination of electrical resistivity of dry coke beds. Metall Mater Trans B 39(1):7–15
6. Eidem PA, Tangstad M, Bakken JA (2008) Determination of electrical resistivity of dry coke beds. Metall Mater Trans B 39B:7–15
7. Surup GR, Pedersen TA, Chaldien A, Beukes JP, Tangstad M (2020) Electrical resistivity of carbonaceous bed material at high temperature. Processes 8(8):933
8. Barker I, Rennie M, Hockaday C, Brereton-Stiles P (2007) Measurement and control of arcing in a submerged-arc furnace. In: Proceedings of the INFACON XI. New Delhi, India, pp 685–694
9. Steenkamp JD, Hockaday CJ, Gous JP (2016) Analysis of electrical energy dissipation in submerged-arc furnaces producing silicomanganese. In: 11th European electric steelmaking conference & expo (EEC2016), Venice, Italy, pp 1–11
10. Dijks H, Smith D (1980) Factors affecting the resistivity and reactivity of carbonaceous reducing agents for the electric-smelting industry. J S Afr Inst Min Metall 80:286–296
11. Surup GR, Smith-Hanssen N, Tangstad M (2021) The properties of carbon blends in submerged arc furnaces. In: Proceedings of the 16th international ferro-alloys congress (INFACON XVI), Trondheim, Norway, pp 1–11
12. Gaal S, Lou D, Wasbø S, Ravary B, Tangstad M (2015) Melting phenomena in ferromanganese production. In: Proceedings of the INFACON XI. New Delhi, India, pp 247–257
13. Ringdalen E, Gaal S, Tangstad M, Ostrovski O (2010) Ore melting and reduction in silicomanganese production. Metall Mater Trans B 41B:1220–1229
14. Safarian J, Kolbeinsen L (2008) Kinetic of carbothermic reduction of MnO from high-carbon ferromanganese slag by graphite materials. ISIJ Int 48(4):395–404
15. Safarian J, Tangstad M (2010) Slag-carbon reactivity. In: INFACON XII, Helsinki, Finland
16. Eidem PA (2008) Electrical resistivity of coke beds. PhD thesis, Norwegian university of science and technology, Trondheim, Norway, ISBN 978-82-471-1258-8
17. Miyachi Y, Mochida M, Fuchi Y (2001) High thermal electrical property of manganese ore in the production of high carbon ferromanganese. In: Proceedings of the INFACON IX, Quebec City, Canada, pp 236–243
18. Monsen B, Tangstad M, Solheim I, Syvertsen M, Ishak R, Midtgaard H (2007) Charcoal for manganese alloy production. In: Proceedings of the INFACON XI, New Delhi, India, pp 297–310
19. Monsen B, Tangstad M (2004) Use of charcoal in silicomanganese production. In: Proceedings of the INFACON X, Cape Town, South Africa, pp 392–404